J. Indian Inst. Sci.
A Multidisciplinary Reviews Journal
ISSN: 0970-4140 Coden-JIISAD

REVIEW ARTICLE

Flash Boiling in Sprays: Recent Developments and Modeling

*Bharat Bhatia and Ashoke De**

Abstract | This study aims to cover the modeling of flash boiling effects in the sprays. There is a lack of an economical and computationally efficient methodology to analyze this complex phenomenon. Flash boiling being an essential phenomenon in combustion engines is the cause of change in the spray structure, cone angle, liquid penetration length, droplet distribution, etc. The paper revisits various models used to capture the effect of the flash boiling phenomenon and identifies the drawbacks and challenges, respectively. The whole phenomenon is divided into various stages and discussed stepwise. It tries to address the issues related to the gaps in modeling.

1 Introduction

There has been a considerable effort in modeling the atomization processes in different regimes of the spray. The sprays can either be injected as a solid jet or as a hollow cone, depending on the application—gas-turbine jet engine, gasoline engine, diesel engine or spray cooling, painting, humidifiers. The atomization process and the resultant droplet traits, i.e., size, distribution, velocity, etc., play an important role in each and every case. In case of combustion engines, the liquid fuel is required to disintegrate into very small droplets in a short duration, to provide larger surface area for the rapid evaporation and quick mixing with the surrounding air.

From the perspective of the physics of breakup, the spray structure is divided into two major zones—primary and secondary breakup zones. The modeling of the small primary breakup is more challenging than the secondary breakup regime, due to its close vicinity to the injector and several factors involved in the instability of the liquid core/sheet. In the case of combustion engines, the continuous heating of the combustion chamber heats up the chamber walls, injector ports, injector chambers, nozzle walls, and the surrounding area. When the pressurized liquid fuel enters the injector, it heats up to the superheated temperature. The fuel near the wall may undergo a phase transition, depending on the flow velocity (residence time) of liquid fuel within the injector.

At the time liquid fuel exits the injector nozzles into the combustion chamber, it experiences a drop in pressure. Now, the liquid fuel experiences a combination of three destabilizing forces responsible for the primary breakup: aerodynamic forces by the surrounding gas, forces due to turbulence within the liquid phase and the sudden impulse due to the implosion of cavitation bubbles. There exist two possibilities—first, the pressurized liquid fuel entering the combustion chamber may already contain a portion of gaseous fuel in the form of bubbles formed from earlier phase transition within the injector due to local pressure changes. Once the liquid fuel is in the combustion chamber, the bubble experiences compressing forces, and the implosion of the bubble occurs resulting in the disintegration of the liquid sheet or droplet into yet smaller droplets. It is the cavitation-based atomization. The second possibility is that superheated pressurized liquid fuel enters the low-pressure combustion chamber and suddenly flashes into tiny droplets and gaseous fuel. The latter case does not necessarily be a multiphase flow prior to combustion chamber entrance. This process is commonly referred to as a flash boiling phenomenon.

In the present work, the authors have presented a review of the flash boiling phenomenon in detail, to not only understand its physics but also to contribute to the gaps left to bridge.

Department of Aerospace Engineering, Indian Institute of Technology, Kanpur 208016, India.
**ashoke@iitk.ac.in*

2 Flash Boiling Atomization

Although some effort has been made to understand and mathematical modeling of flash boiling and cavitation in sprays, significant research study is still required to explain this complex multiphase phenomenon. The whole process from its initiation to the completion can be divided into three steps: (1) bubble nucleation, (2) bubble growth, (3) breakup due to bubble burst or micro-explosion.

3 Bubble Nucleation

It is the first step toward the start of the flash boiling phenomenon when the bubble nucleates in the liquid fuel core. There are two possible mechanisms for bubble nucleation—homogeneous nucleation and heterogeneous nucleation.

Homogeneous nucleation is the situation when the bubble is formed entirely within the liquid, and the impurity, dissolved gases, and/or wall plays no role in its formation. For a liquid in a container, the contact angle of the liquid phase with surface should be zero. When the bubble formation takes place at the interface of liquid and surface, or at the interface with the impurity, it is termed as heterogeneous nucleation. The contact angle of the volatile liquid is greater than zero for the latter case. Also, the latter case is reported to have more violent boiling than its counterpart[1].

4 Theory for Bubble Nucleation

As explained by Blander and Katz[1], an absolute maximum of minimum work is required to create a surface of the bubble and transfer molecules from liquid to bubble. This work will increase to infinity as the bubble increases in size, hence rendering it unstable and consequently causing bubble collapse. Thus, it is impossible to boil the liquid at its boiling point under the conditions where the liquid has zero contact angle with the container surface. If the liquid is superheated, the work to transfer molecules from liquid to gas becomes negative and the total minimum work done (including work done to create the bubble surface) is as shown in Fig. 1. This can be attributed to the decrease in surface tension and an increase in vapor pressure. The maxima of work acts as a barrier after which boiling occurs and the growth of the bubble is self-sustaining. This boiling initiation for a given ambient pressure takes place at a range of temperatures in the superheated regime. The maximum point of superheating of a liquid is denoted by point C in

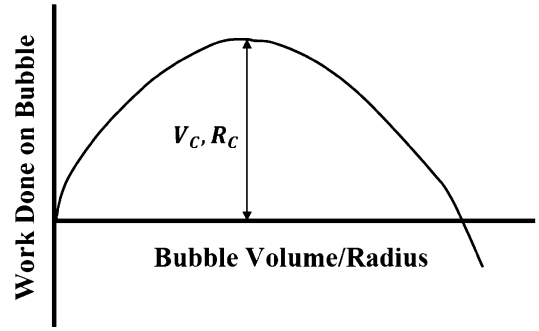

Figure 1: Work required to form a bubble as bubble volume increases. Critical bubble volume/radius is the barrier for the formation of the bubble[1].

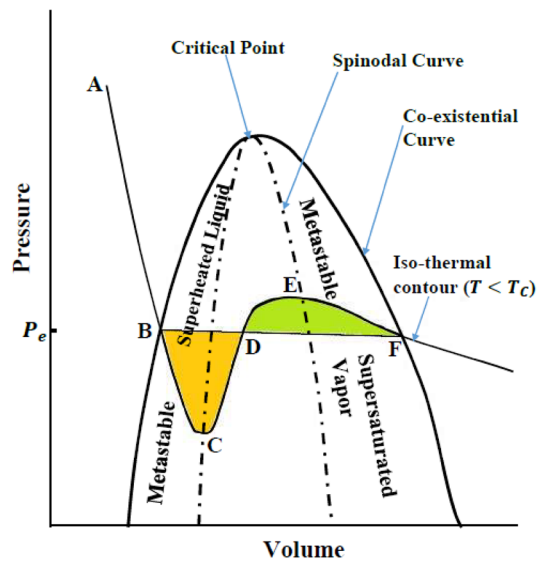

Figure 2: Pressure–volume phase diagram showing true isothermal contour. Point C represents the limit of superheat[1].

Fig. 2, which is the true limit of superheating[1]. For different values of temperature, less than the critical temperature, this point traces the spinodal line that divides superheated/metastable liquid and the unstable region as shown in Fig. 2.

The theory on bubble nucleation has been developed by researchers in the past[1–6]. The modified version [7–9] of a generalized form of the bubble nucleation equation as proposed by Blander and Katz[7] is

$$J = N_0 k_f \exp\left(-\frac{\Delta A^*}{kT}\right), \tag{1}$$

where work maxima or the barrier, usually termed as activation energy for the bubble to grow, is expressed as

$$\Delta A^* = \frac{16\pi\sigma^3}{3(P-P_0)^2}. \tag{2}$$

Equation 1 approximates the number of bubbles nucleated in the liquid fuel when it enters the combustion chamber, since the number of bubbles nucleated and the critical diameter of the smallest bubble will influence the primary breakup phenomenon. Yet, the critical diameter of these bubbles, which have crossed the barrier and are self-sustaining, is unknown. The necessary derivation of the expression along with basic reasoning for the critical diameter of the bubbles nucleated in the liquid fuel core is shown below.

The homogeneous nucleation rate, as discussed above, depends on the degree of superheating, which in turn is responsible for the flashing of the liquid fuel. Here, the essential derivation of the process which is elaborated below happens simultaneously with the aerodynamic breakup. The dominance of a mechanism is determined by the smaller breakup characteristic time out of the two parallel mechanisms[10].

In the experiments, Shepherd and Sturtevant[11] observed single-bubble formation within the butane droplets during flash boiling. If the thermodynamic equilibrium is considered during the nucleation process, the pressure difference (between droplet pressure and the ambient pressure) balances the pressure due to surface tension.

$$(P_d - P_{\text{amb}})\pi D_d^2/4 = \pi D_d \sigma. \tag{3}$$

Hence, the droplet pressure becomes:$P_d = P_{\text{amb}} + 4\sigma/D_d$

For bubble growth or internal boiling, $P_d < P_{\text{sat}}(T_d)$ ([12]as cited by[10]). It is assumed that vapor pressure P_v or pressure within bubble P_b approximates the slope along the vapor pressure curve ($P_v(T_v)$) in the phase diagram. According to Lanello[13], as referred in[10], from the above equation and the Clausius–Clapeyron equation along the vapor-pressure curve,

$$T_l - T_v = \frac{\mathcal{R}T_l T_v}{h_{fg}M_W}\ln\left[1+\frac{4\sigma}{P_v D_d}\right] \tag{4}$$

The difference in temperatures P_d and P_d is very small and hence the logarithmic part can be approximated linearly. Inequality,

$$\frac{T_d - T_{\text{amb}}}{T_{\text{amb}}} > \frac{T_l - T_v}{T_v} = \frac{1}{C}\left[1+K_e\frac{\rho_l}{\rho_{v,\text{amb}}}\right], \tag{5}$$

where $C^{-1} = \frac{\mathcal{R}T_L}{h_{fg}M_W}$ and $K_e = \frac{4\sigma M_W}{\rho_l \mathcal{R} T_{\text{amb}} D_d}$. For the critical condition, the center temperature of the drop T_d should be equal to the saturation temperature T_{sat}. Hence, the equation becomes

$$\frac{T_{\text{sat}} - T_{\text{amb}}}{T_{\text{amb}}} = \frac{1}{C}\left[1+K_e\frac{\rho_l}{\rho_{\text{vamb}}}\right]. \tag{6}$$

Bushnell and Gooderum[14] showed that the amount of superheating needed was

$$\frac{T_l - T_{\text{sat}}}{T_l} = 0.1 \tag{7}$$

Hence, the threshold condition for bubble formation is obtained for bubble nucleation from Eqs. (6) and (7):

$$T_l = \frac{T_{\text{amb}}}{0.9}\left(1+\frac{1}{C}\left[1+K_e\frac{\rho_l}{\rho_{v,\text{amb}}}\right]\right).$$

It is concluded that $T_d > T_l$.From the above, the critical radius of the bubble can be obtained, using similar calculation as for the droplet, with vapor pressure calculated from above:

$$R_{b,0} = \frac{2\sigma}{P_v(T_d) - P_{\text{amb}}}.$$

In many cases, the critical superheat for nucleation usually ranges from 5 to 15 K[10].

5 Bubble Growth

Once nucleated, the second stage is the bubble growth within the liquid jet core/sheet. There have been attempts to formulate a generalized equation and accurately predict bubble growth[15–17]. The most commonly used is the Rayleigh equation[15].

$$R\frac{\partial^2 R}{\partial t^2} + \frac{3}{2}\left(\frac{\partial R}{\partial t}\right)^2 = \frac{P_v - P_l}{\rho_l}. \tag{8}$$

The left-hand side of the equation shows the inertial effects, while the right-hand side is the pressure difference forcing the bubble growth through the bulk liquid. In a practical situation, the bubble growth process is much more complicated and the above approximation might not be valid.

5.1 Drawbacks of the Equation

The Rayleigh equation is based on some assumptions:

1. The effect of surface tension is neglected. Surface tension plays an essential role in the bubble dynamics, the inclusion of which

in the bubble growth gives rise to the Rayleigh–Plesset equation[16]. It is considered during the nucleation stage of the bubble as described above.

2. Viscous effects are neglected. The surface tension and the surface dilatation, as well as the shear viscous effects, have been included in the modified Rayleigh equation by Scriven[17]. Both the stresses oppose the growth of a bubble. Though the theoretical work of Scriven[17] is applicable to any fluid interface irrespective of its shape, the dynamics equation for the bubble can be deduced as

$$R\frac{\partial^2 R}{\partial t^2} + \frac{3}{2}\left(\frac{\partial R}{\partial t}\right)^2 + \frac{2\sigma}{R\rho_l} + \frac{4\mu V_i}{R} + \frac{4\kappa V_i}{R^2} = \frac{P_v - P_l}{\rho_l} \tag{9}$$

3. The bubble growth happens in the infinite liquid medium. Many applications usually have a gaseous or solid boundary which affects the bubble growth considerably. Further, the curvature of the boundary also contributes to the manner the bubble evolves. For example, bubble growth near a free surface will be different from the one within a ligament or a droplet.
4. There is no mass transfer with the surrounding liquid across the bubble surface. There could be two instances where mass transfer calculations would be of use. The first is for accurate prediction. In the case of flash boiling of a minimal amount of the liquid, as may be the case with bubble within a droplet, any loss of mass by the liquid and gain of the mass of the vapor bubble can be considered. A correct prediction of the liquid mass in the bubble–droplet system undergoing flash boiling will help predict the size of child droplets accurately.
   Secondly, it is highly possible that the bubble growth may be controlled by the mass transfer diffusion from the bulk liquid to the vapor bubble as in the case of binary solutions, having components of different volatility. In the case of supersaturated binary solutions, a low volatile solute in a relatively non-volatile solvent would start to nucleate in the conditions of heating or depressurization. A mass transfer equation needs to be solved coupled with the bubble growth equation, Eq. 9. A model for mass diffusion-controlled bubble growth has been developed by[18–22] for the supersaturated binary mixtures. In this study, mass transfer is assumed to happen across an approximated boundary layer surrounding the bubble. Payvar[19] also considered the convection effect in mass diffusion. Arefmanesh[20] (as referred by[22]) used an exact concentration profile for solving the equations of mass diffusion-induced growth of the bubble in a viscous liquid. Mass diffusion effect would be a driving force for bubble growth in the study of binary mixtures such as biofuels. There have been studies involving a mixture of ethanol and gasoline[23–25].
5. The thermal effects are not considered in the above equation. It is crucial in the sense that through it, the variation in the liquid properties with temperature is captured. To include the effects of changing thermal conditions throughout the growth process of a bubble, Forster and Zuber[26] coupled the energy equation with the modified Rayleigh equation. Adding the energy equation allows observing the change in the rate of bubble growth in the superheated liquid. As the bubble grows, the temperature of the superheated liquid surrounding the bubble decreases, and there is change observed in the temperature distribution in that liquid[27].

As indicated by Lee and Merte[28] and in other subsequent works[29–31], the bubble growth can be divided into three stages: initial surface tension-controlled stage, pressure difference or inertia-dominated stage, and finally the heat transfer-controlled stage. The first stage, dominated by the surface tension stresses, is mostly insignificant to be considered of any practical interest majorly due to the timescales related to it[28]. At this stage, the bubble is of the order of critical size. In the second stage, inertial forces dominate the bubble growth process, though other stresses are still in action. This is due to the increased magnitude of the acceleration of the bubble interface in the bulk liquid. The third stage is controlled by the energy transfer process. The details of all the three stages are discussed below.

Experimental results of Lien[32] shows that the second stage dominates the bubble growth in the system at a low pressure of 0.01 atm with water, and the Rayleigh equation, Eq. 8 shows a good match with this experimental data. For the inclusion of the third stage of heat transfer during the bubble growth, Plesset and Zwick[33] considered a thin thermal boundary layer around the bubble.

They provided a zero-order solution to the energy equation for bubble wall temperature as

$$T_b = T_{l,\text{bulk}} - \left(\frac{\alpha}{\pi}\right)^{1/2} \int_0^t \frac{R^2(x)\left(\frac{\partial T}{\partial r}\right)_{r=R(x)}}{\left(\int_0^t R^4(y)\,\mathrm{d}y\right)^{1/2}}\,\mathrm{d}x. \tag{10}$$

Here, the heat source term is not considered as mentioned in[33]. Later, Plesset and Zwick[34] formulated a solution (Eq. 11) for the vapor bubble growth using the same zero-order solution. This solution proved to be valid only for times when the vapor bubble is dominated by the heat transfer process. Thus, except for the last stage, the velocity of bubble growth was much smaller in the first two stages. In the later work by Prosperreti and Plesset[35], the results of both the inertia-dominated equation and Eq. 10 along with exact vapor pressure curve were in a good match with that of Donne and Ferranti[36]. Though the results were off for the lower values of superheat because thin boundary layer assumption is not valid for this case.

$$\frac{\mathrm{d}R}{\mathrm{d}t} = \frac{1}{2}\left(\frac{12\alpha_1}{\pi t}\right)^{1/2} \frac{\rho_l c_l (T_{\text{amb}} - T_{\text{sat}})}{\rho_v h_{fg}}. \tag{11}$$

With this, the solution to the bubble growth was made into a two-step process to get reasonable results. Mikic et al.[37] later solved both the energy and the momentum equations along with the Clausius–Clapeyron equation and combined it with the Rayleigh equation (Eq. 8). The solution of the equation provided a single expression for both the stages given in non-dimensional form as:

$$R^+ = \frac{2}{3}\left[(t^+ + 1)^{3/2} - (t^+)^{3/2} - 1\right] \tag{12}$$

where $R^+ = \frac{R}{B^2/A}, t^+ = \frac{t}{B^2/A^2}, A = \left(\frac{2\Delta T h_{fg}\rho_v}{3T_{\text{sat}}\rho_l}\right)^{1/2}$ and $B = \left(\frac{12Ja^2\alpha_l}{\pi}\right)^{1/2}$. Theofanous and Patel[38] also used a similar methodology as that of Mikic et al.[37] except they used linear vapor pressure relation instead of the Clausius–Clapeyron equation. A scaled modified closed-form expression of Mikic et al.[37] was also suggested and given as:

$$R^* = \frac{2}{\pi^2}(2/3)^{1/2}\left[(\frac{1}{2}\pi^2 t^* + 1)^{3/2} - (\frac{1}{2}\pi^2 t^*)^{3/2} - 1\right], \tag{13}$$

where $R^* = \mu^2 \frac{R}{R_C}$, $t^* = \beta\mu^2 t$, $\mu = \frac{1}{3}\left(\frac{2\sigma\alpha}{\pi}\right)^{1/2} \left(\rho_v \frac{h_{fg}}{k(T_{l,\text{bulk}} - T_{\text{sat}})}\right)\left\{\rho_v[P_v(T_{l,\text{bulk}}) - P_{l,\text{bulk}}]\right\}^{-0.25}$ and $\beta = \frac{(P_v(T_{l,\text{bulk}}) - P_{l,\text{bulk}})^{3/2}}{2\sigma\rho_l^{1/2}}$. Lee and Merte[28] also solved the two equations, namely momentum and energy, simultaneously along with the vapor pressure curve. They found that the scaled modified form of a solution by Mikic et al.[37] was in good agreement with the results of their numerical computations and many other experimental results. It is bound to perform better because the effect of both the heat diffusion and the inertial effects has been included during the derivation of the solution. Lee and Merte[28], as in the previous cases, had to provide some initial perturbation to start the bubble growth. They concluded that the disturbance did not have any significant effect on the bubble growth for moderate to high superheat degrees, except in the case of low superheat levels where initial disturbance should be sufficiently small which otherwise changes the bubble growth delay time.

Hence, the large values of liquid superheat or low system pressure causes the bubble growth to become inertia controlled, while for lower levels of liquid superheats or high system pressure the bubble growth is dominated by the heat diffusion process[28]. Further, Lee and Merte[29] conducted the experimental study on vapor bubble growth in microgravity on R113 and compared the results with their closed form expression of superheat model with uniform as well as non-uniform initial temperature distribution. It is different from a few studies mentioned earlier with respect to the temperature profile taken around a growing bubble[28], [36]. Similarly, Theofanous et al.[39] and Board and Duffy[40] had assumed the temperature profile for numerical modeling as compared to Lee and Merte[29]. The expression used by Lee and Merte[29] in their work is given by

$$T(r, t_{dh}) - T_{0,\text{bulk}} = \frac{2q_l''\sqrt{(\alpha t_{dh}/\pi)}}{k_l}\exp\left(\frac{-r^2}{4\alpha t_{dh}}\right) - \frac{q_l'' r}{k_l}\operatorname{erfc}\left(\frac{r}{2\sqrt{\alpha t_{dh}}}\right). \tag{14}$$

Later, Robinson and Judd[30] performed a detailed numerical study of various stages of bubble growth in an infinite pool of liquid. They looked into the effect of changing the initial superheat and system pressure on the bubble growth characteristics by solving the one-dimensional energy equation. For a spherically symmetric bubble, the rate of increase of its size is related to the amount of heat diffused through the interface,

$$\frac{\mathrm{d}R}{\mathrm{d}t} \approx \frac{1}{\rho_v h_{fg}}\left(k_l \frac{\Delta T(t)}{\delta_{th}(t)}\right), \tag{15}$$

where $\Delta T = T_{\text{inf}} - T_v$ is the temperature difference across the interface, and δ_{th} is the thickness of

the thermal boundary layer surrounding the bubble. The amount of heat transferred is the driving force throughout the bubble growth process. Secondly, they considered the inertial resistance as the hydrodynamic force at the bubble–liquid interface given by

$$P_{hd} = \rho_l R \frac{\mathrm{d}^2 R}{\mathrm{d}t^2} + \rho_l \frac{3}{2}\left(\frac{\mathrm{d}R}{\mathrm{d}t}\right)^2. \tag{16}$$

The pressure (P_l) exerted by the liquid at the interface is the sum total of the static (P_∞) and the hydrodynamic pressure (P_{hd}). As mentioned previously about the initial stage of bubble growth, the surface tension plays a governing role till the interface acceleration (or the hydrodynamic force) reaches its maxima. In this zone, a small increase in radius leads to the decrease in the vapor pressure within the bubble. According to the equation of state, there is a simultaneous decrease in the temperature within the bubble. The heat transfer increases from the surrounding liquid into the bubble with a higher temperature difference across the interface. As mentioned by Robinson and Judd[30], there is an established thermal feedback effect which ensures that the bubble acceleration continuously increases to its maxima. Figure 3 shows the details of variation of the stress as the bubble grows in the bulk liquid.

This is the moment, when hydrodynamic forces take a lead role in controlling the bubble growth, as they resist the motion of the interface. The hydrodynamic forces adversely affect the thermal feedback and prevent the increased heat transfer from outside. Though the bubble still grows, the acceleration of interface decreases to nil with time. As mentioned by[30], the thickening of the thermal boundary layer by advection and conduction tends to decrease the heat flux at the interface and the consequent effect on bubble growth. The radial outward motion of the bubble tends to push the fluid in the thermal boundary layer into the bulk liquid, while the heat is conducted from the hottest region in the thermal boundary layer near the interface into the bubble. This leads to increment of the thickness of a thermal boundary layer, further decreasing the heat flux.

When the thermal boundary layer has increased to its considerable size, the growth of bubble slows down and is limited by the rate of liquid evaporated into the vapor. The pressure difference across the interface at this stage is almost zero. Also, the temperature difference also remains insignificant, and the heat transfer process or the thermal boundary layer

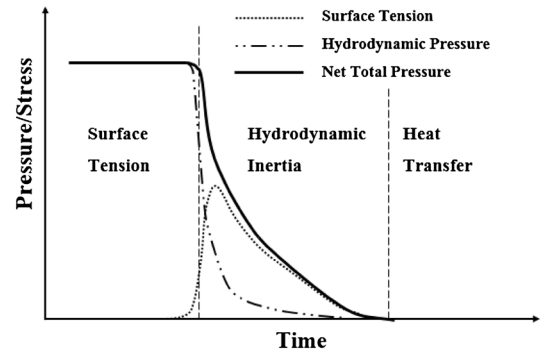

Figure 3: Various regimes of bubble growth dominated by different forces/stresses[30].

plays a dominating role. Here, the data of Robinson and Judd[30] agrees well with zero-order analytic expression by Plessent and Zwick[34]: $\delta(t) = (1/3\pi\alpha t)^{1/2}$, whose theory is completely based on the thermal boundary layer.

These observations of the bubble growth process indicate that variation in the liquid properties needs to be considered at every stage with changing temperature and other field variables[31].

6 Micro-Explosion

The third and the least understood stage is the 'micro-explosion,' which actually defines the flash boiling process. It is also referred to as 'bubble boiling explosion,' 'contact vapor explosion'[1] or 'bubble burst.' Some of the facets of this complex process that still pose a challenge in mathematical modeling are the criterion for the breakup initiation, the number of child droplets formed after the breakup, size distribution and the velocity of the child droplets. Once these parameters are known, other broader details like the amount of vapor release in the process can be found out quickly. A schematic of micro-explosion process is shown in Fig. 4, which gives a rough idea of the number of parameters needed to be calculated.

There have been experimental studies by Oza and Sinnamon[41] and Oza[42], describing the two regimes of jet atomization. In one of the regimes, the spray cone angle remains unchanged while flashing of liquid fuel occurred within the nozzle. In the second regime, the chamber pressure is low enough to cause the external expansion of the two-phase fluid ejecting from the nozzle, consequently increasing the spray cone angle. The former case lies in a low superheat zone, while the latter lies in a high superheat regime. According to[41], the bubble growth process occurs in both the cases, but in the latter case the process

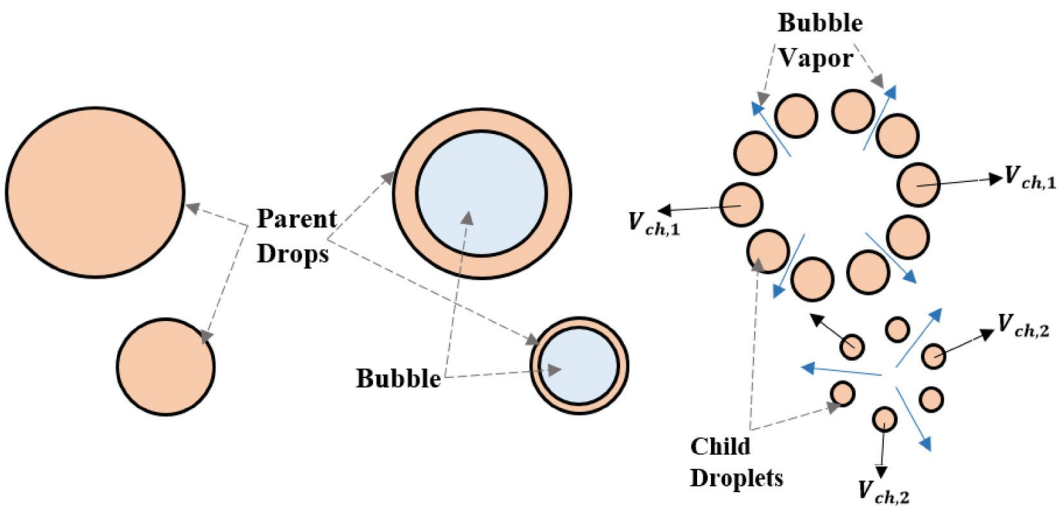

Figure 4: Schematics of micro-explosion of a bubble-within-a-droplet system resulting in the formation of secondary droplets.

continues outside the nozzle, into the chamber. However, the experiments conducted by Reitz[43] shows that the liquid core remains intact even outside the nozzle when the experimental conditions lie in the internal flashing regime of Oza and Sinnamon[41]. Reitz[43] used "high intensity, short duration, backlit, spark photographs" for capturing the liquid core. Reitz[43] blamed the light scattered from the flash boiling spray plume for the obscurity of the liquid core, which prevented Oza and Sinnamon[41] from capturing it. Thus, the atomization of the superheated liquid happens outside the nozzle. Senda et al.[44] studied the spray characteristics in flash boiling conditions such as increase in spray angle, shortening of liquid core length and narrower droplet size distribution with an increase in the superheat degrees.

Many models have been suggested to date by Sher and Elata[45], Razzaghi[46], Senda et al.[44], Zeng and Lee[8] and Shen[9], which are covered below.

Sher and Elata[45] assumed that the bubble burst happens at the instant when the bubbles form a close-packed array, touching each other. According to this theory, a continuous liquid with separated bubbles changes into bubbles with separated liquid droplets at the time of bubble burst. A part of the energy of the bubble becomes the energy of the child droplets formed after the bubble burst. In this assumption of a close-packed array, the fraction of vapor mass and liquid mass is $\varpi/6$ and $1-\varpi/6$, respectively. Thus, the mass of the liquid at the time of bubble burst is,

$$\mathcal{M} = \rho_l(1-\pi/6). \tag{17}$$

The assumption of child droplets to follow log-normal distribution as per their experiments and, from the continuity equation, the number of secondary droplets formed after the bubble burst is given as:

$$n = \frac{1-\pi/6}{(\pi/6)D_{50}^3 \exp(4.5\ln^2\sigma_g)}. \tag{18}$$

Razzaghi[46] developed a model for breakup and atomization of the jet. He considered both the aerodynamic and flash boiling as the reasons for the breakup. The primary droplets are presumed to be formed from the liquid core due to aerodynamic disturbances, and flash boiling starts in these droplets. Two regimes of bubble growth have been considered—inertia and heat transfer control. When the wavelength of instability on the droplet surface is five times the film thickness, the bubble–droplet system becomes unstable[47] and breaks into tertiary droplets. The breakup of the droplets with bubble occurs due to the Rayleigh–Taylor instability. The size of the tertiary (child) droplets is calculated from the mass conservation equation. Moreover, the droplets are assumed to not coalesce because of the high evaporation rates which cause strong repulsive forces among the droplets[48] (as cited by[46]). Though the model concentrates on the minute details of the flash breakup, a number of assumptions limit its use and it needs further improvement.

Senda et al.[44] modeled the flash boiling process with all the three stages. The model is based on the experimental study conducted on *n*-pentane and *n*-hexane using a pintle-type injector, which means the injection pattern manifested

a hollow cone. The number of child droplets is assumed to be twice the bubble density in a parent droplet. Though the calculated child droplet size was near the measurements, the data points were too less to verify the model. A maximum value of void fraction ($\varepsilon = 0.45$) is used to predict the instant of initiation of the third stage, i.e., the micro-explosion.

The assumption of a void fraction as being the deciding factor for bubble burst has also been used by Adachi et al.[49] is $\varepsilon = 0.45$, Kawano et al.[50] is $\varepsilon = 0.55$. The void fraction value was based on the experiments conducted by Suma et al.[51], where it ranged between 0.51 and 0.53.

Similar to[46], a model based on the linear instability analysis was proposed by Zeng and Lee[8]. The micro-explosion, in this case, happens when the instabilities along the bubble and the droplet surfaces grow more significant than the characteristic length of the spray. The characteristic length is equal to the film thickness of the droplet. The case is similar to[46] concerning the instability of the droplet film being the cause of micro-explosion and both the models consider an aerodynamic breakup. In this model, the velocity of the child droplets is also calculated along with its size using the conservation equations. The breakup criteria of this model are set as:

$$C(t_b) = \frac{R_{d0} e^{\int_0^t b\omega dt}}{R_d - R_i} = C_{\text{crit}}. \tag{19}$$

$C_{\text{crit}} = 5$ is taken according to the experimental results. The perturbation equations (derived from the governing equations) are solved along with a pressure perturbation relation of the bubble. The pressure perturbation within the bubble is related to the bubble radius perturbation by the sound speed inside the bubble. The final instability equation is solved for the disturbance growth rate given in[8]. The child droplet size, velocity and the number of secondary droplets are calculated from the governing equations of mass, momentum and energy. The droplet size and velocity of the child droplet are given as:

$$R_{32,\text{ch}}^{-1} = B\frac{R_d^2 + R_i^2}{R_d^3 - R_i^3} + \left(\frac{3}{2}\frac{R_d^4(R_i^{-1} - R_d^{-1})}{R_d^3 - R_i^3}V_i^2 - \frac{V_b^2}{2}\right)\frac{\rho_l}{3\sigma}, \tag{20}$$

$$V_{\text{ch}} = \frac{3R_i^2 V_i (R_d - R_i)}{R_d^3 - R_i^3}. \tag{21}$$

The droplets are assumed to have χ^2-distribution. Similarly, the breakup characteristics of the flash boiling are compared with the aerodynamic breakup, as both happen at the same moment. In this study, the superheat degree varies from 4 to 64 K. However, they solved the bubble growth without considering the energy equation.

Similarly, Shen[9] 's model is based on the conservation of the surface energy of liquid droplets. In this case, the minimal total surface energy is the breakup criterion of the model. The spontaneity of the event has been related to the Gibbs free energy of the bubble–droplet system. Both of the last models have been used for multi-component fuels[9, 52].

7 Alternative Flash Boiling Models

There are other alternative flash boiling models suggested by Brown and York[53], Lienhard and Stephenson[54], Gooderum and Bushnell[55], Lienhard and Day[56], Crowe and Comfort[57], Kitamura et al.[58], Zuo et al.[59] and Khan et al.[60]. These models are empirical or semi-empirical formulations and do not explain the complete physics behind the process, few of which are discussed below.

Brown and York[53] proposed a critical Weber number corresponding to a superheat degree, above which flash atomization occurs. The value is based on the correlated data for superheated water, Freon-11 and water through which carbon dioxide was bubbled. The critical value is defined as:

$$We_j = \frac{1}{2}\frac{\rho_{\text{air}} u_0^2 D_j}{\sigma_L} \tag{22}$$

The corresponding critical superheat degree[10, 53],

$$C_{\text{bub}}\Delta T^* = \begin{cases} 0.100 - 2.95 \times 10^{-3} We_j & \text{if } We_j \le 12.5 \\ 0.0584 - 2.13 \times 10^{-3} We_j & \text{if } We_j \ge 12.5. \end{cases} \tag{23}$$

Here, $C_{\text{bub}} = Ja(\pi\alpha)^{1/2}$ is the bubble growth rate. Similarly, the droplet size correlated with critical Weber number or jet velocity was proposed as[10, 53]:

$$R_d = \begin{cases} \frac{c_1 - c_2}{We_j} B_G & \text{if } B_G \ge B_{\text{crit}} \\ \frac{12.5}{2 \times We_j} D_j & \text{if } B_G \le B_{\text{crit}}. \end{cases} \tag{24}$$

Here, $B_G = Ja(\pi\alpha)^{1/2}/\Delta T$ is the bubble growth rate constant, $B_{\text{crit}} = 0.0584 - 2.13 \times 10^{-3} We_j$ is the critical bubble growth rate condition and constants $c_1 = 0.87 \times 10^{-3}$ and $c_2 = 5.709 \times 10^{-3}$

[10]. Lienhard and Day[56] established the condition and average length of liquid core breakup as:

$$L_{\text{break - up}} = V_j(\bar{t}_{d1} + t_{d2}). \tag{25}$$

Kitamura[58] found a critical superheat for the flashing breakup, expressed as the Jacob Number, corrected with a correction factor, ϕ, as a function of jet Weber number. In this Weber number, vapor density is used in place of air density. The empirical relation is:

$$\phi Ja = 100 We_j^{-1/7}, \tag{26}$$

$$\phi = 1 - \exp\left(\frac{-2300}{\rho_l - \rho_v}\right). \tag{27}$$

Both Brown and York[53] and Kitamura[58] models are not applicable to low Weber number jets.

Zuo et al.[59] cover several aspects in their model: transient conduction limiting sheet flash vaporization model, an effect on the primary breakup model, superheat flash vaporization and heat transfer model for drops and Stefan flow model. First, the transient conduction sheet flash vaporization model solves one-dimensional energy equation to calculate the temperature distribution within the spray sheet. From this, the evaporation rate can be calculated, considering the radial decrease in the sheet thickness. Second, it assumes primary breakup due to aerodynamic instability. The linearized stability atomization (LISA) model[61] is modified for superheating conditions which include the change in primary (child) droplet size and the spray cone angle. The drop size correlation is based on the experimental results of VanDerWege[62], [63] and Reitz[43]. To take into account the flash boiling effect on the spray droplets in their third model, the heat transfer from the droplet interior to its surface, along with the heat transfer from the surrounding gas at a higher temperature to the same droplet surface is considered. The net heat transferred gives the total evaporation rate of the droplet due to flash boiling. Last, the Stefan flow is also modeled as the blowing effect due to high evaporation rates and mass transfer with the external flow will give way to a thick boundary layer surrounding the droplet.

For flashing releases, Cleary et al.[64], Witlox et al.[65] developed an empirical sub-model to predict the droplet size and its distribution. It includes mechanical breakup based on the critical Weber number and transitions between flashing and non-flashing jets. The results were overpredicted in some cases and needed further investigation.

A model by Khan et al.[60] developed for flash boiling in gasoline direct injection (GDI) sprays uses surface tension energy change, from the parent bubble–droplet system to the child droplets, for the calculation of child droplet size, velocity and spray cone angle.

The empirical or semi-empirical relations are limited to some specific cases and hence cannot be generalized. They not only lack the explanation of the physics behind the process, but also consequently demand a more experimental investigation for mining any further details.

There has been considerable work[22, 62–68] on the effervescent atomizer designs and two-phase flows, which have a significant role in case of high superheat conditions. Since the present work concentrates on the review of the basic physics of the flash boiling process in sprays, which is common to any application, specific topics such as the atomizer/vessel design pertaining to some industrial application have not been covered.

8 Conclusion

There has been considerable improvement in modeling the flash boiling process and its feasibility, especially concerning the initial stage of bubble nucleation and growth. In practical problems, even the studies involving models with the most detailed physics underperform on many fronts. The factors for the failure mainly pertains to a large number of assumptions and limitations of a given model. This work tried to provide an insight into the modeling efforts of the past and their respective drawbacks. There still remains a lot of work to be done experimentally, analytically and computationally to develop a generalized formulation for flash-boiling.

Based on the review of various models and the experimental results witnessed, some of the following conclusions can be made:

1) In all the computational studies, homogeneous nucleation is considered. The heterogeneous nucleation of bubble is dominant in the lower superheat regime and should be considered in the computational as well as analytical studies. This might answer the two-phase flow just at the liquid jet exit.
2) As it has been aforementioned, the three regimes of bubble growth play an important role in accurate prediction of bubble life time, which eventually affects the time instant of micro-explosion.

3) As per the bubble growth is considered, it would be different in the liquid core as compared to the liquid droplets. Thus, the surrounding liquid and the free surface curvature of the liquid needs to be included in the calculations.
4) In the event of micro-explosion, the child droplet size, its distribution and the velocities are an important aspects which should be taken into account for better prediction of spray angle and liquid penetration. These factors are also significant with respect to the spray combustion studies where the flame ignition, lift-off height, temperature distribution and emission are important.
5) The empirical or semi-empirical models for micro-explosion or the bubble burst phenomena have found very limited application for their lack of universality for liquid sprays in varied conditions. On the other hand, a very few number of processes are explained by the models physically.
6) Lastly, there have been scant experimental studies which concentrate on the primary break-up due to flash-boiling. It is due to the sophisticated set-up and expensive equipment costs, there is lack of photographic studies of bubble growth in the liquid core and the subsequent bubble burst phenomena, followed by break-up.

Abbreviations

c: Specific heat constant; D: Diameter (of droplet or bubble); h_{fg}: Latent heat constant; J: Number of bubbles per unit volume; Ja: Jacob number; k: Boltzmann constant; k_f: Total evaporation rate of molecular species which forms bubble; k_l: Thermal conductivity of liquid; n: Number of droplets per micro-explosion; N_0: Number density of liquid, (6.023×10^{23}/liquidmolarvol.); M_W: Molecular weight; $\mathcal{M}$: Mass flow rate (for liquid phase); P: Pressure; q_l'': Heat flux to the liquid; r : Radial coordinate; $\mathcal{R}$: Universal gas constant; R: Radius (of droplet or bubble); t: Time; t_{dh}: Dwell time between onset of heating and bubble nucleation; $\bar{t}_{d1}$: Average dwell time between jet ejection and bubble nucleation; t_{d2}: Dwell time for bubble growth after which it bursts (or bubble lifetime); T: Temperature; We: Weber number.

Greek

α: Thermal diffusivity; ε: Void fraction of droplet (R_b^3/R_d^3); κ: Coefficient of dilatation viscosity; μ: Coefficient of shear viscosity; ρ: Density; σ: Equilibrium surface tension; σ_g: Equilibrium surface tension; ω: Angular frequency of disturbance (Eq. 19).

Subscripts

0: Initial state; amb: Ambient state; bulk: Bulk state of the liquid; b: Bubble; d: Droplet; ch: Child droplet; i: Bubble–liquid interface; j: Liquid jet; l : Liquid state; sat: Saturated state; v: Vapor state.

Publisher's Note

Springer Nature remains neutral with regard to jurisdictional claims in published maps and institutional affiliations.

Received: 25 January 2019 Accepted: 8 February 2019
Published online: 21 February 2019

References

1. Blander M, Katz JL (1975) Bubble nucleation in liquids. AIChE J 21(5):833–848
2. Volmer M (1926) Nucleus formation in supersaturated systems. Z Phys Chem 119:277–301
3. Farkas L (1927) The velocity of nucleus formation in supersaturated vapors. J Phys Chem 125:236
4. Becker R, Doring W (1954) Kinetic treatment of the nucleation in supersaturated vapors. Technical Memorandum 1374, NACA-TM-1374
5. Zeldovich YB (1943) On the theory of new phase formation: cavitation. Acta Physicochem USSR 18:1
6. Kagan Y (1960) The kinetics of boiling of a pure liquid. Russ J Phys Chem 34:42–46
7. Avedisian CT, Glassman I (1981) High pressure homogeneous nucleation of bubbles within superheated binary liquid mixtures. J Heat Transfer 103(2):272–280
8. Zeng Y, Lee CFF (2001) An atomization model for flash boiling sprays. Combust Sci Technol 169(1):45–67
9. Shen C (2016) Modeling of biofuel-diesel multi-component fuel effects on vaporization, micro-explosion and combustion. Doctoral dissertation, University of Illinois at Urbana-Champaign
10. Johnson DW, Woodward JL (2010) Release: a model with data to predict aerosol rainout in accidental releases, vol 24. Wiley, New York
11. Shepherd JE, Sturtevant B (1982) Rapid evaporation at the superheat limit. J Fluid Mech 121:379–402
12. Gyarmathy G (1982) The spherical droplet in gaseous carrier streams: review and synthesis. Multiph Sci Technol 1(1–4):99–279

13. Lannello VG. 13. Wallis, and 1', Rothe H (1988) Technical memorandum, liquid release, Final Report. CREARE, Inc., for CCPS, TM-1274 Rev. 8, Project 7230, Nov
14. Bushnell DM, Gooderum PB (1968) Atomization of superheated water jets at low ambient pressures. J Spacecr Rockets 5(2):231–232
15. Rayleigh L (1917) On the pressure developed in a liquid during the collapse of a spherical cavity. Lond Edinb Dublin Philos Mag J Sci 34(200):94–98
16. Plesset MS (1949) The dynamics of cavitation bubbles. J Appl Mech 16:277–282
17. Scriven LE (1960) Dynamics of a fluid interface equation of motion for Newtonian surface fluids. Chem Eng Sci 12(2):98–108
18. Rosner DE, Epstein M (1972) Effects of interface kinetics, capillarity and solute diffusion on bubble growth rates in highly supersaturated liquids. Chem Eng Sci 27(1):69–88
19. Payvar P (1987) Mass transfer-controlled bubble growth during rapid decompression of a liquid. Int J Heat Mass Transf 30(4):699–706
20. Arefmanesh A, Advani SG, Michaelides EE (1992) An accurate numerical solution for mass diffusion-induced bubble growth in viscous liquids containing limited dissolved gas. Int J Heat Mass Transf 35(7):1711–1722
21. Kwak HY, Kim YW (1998) Homogeneous nucleation and macroscopic growth of gas bubble in organic solutions. Int J Heat Mass Transf 41(4–5):757–767
22. Sher E, Bar-Kohany T, Rashkovan A (2008) Flash-boiling atomization. Prog Energy Combust Sci 34(4):417–439
23. Neroorkar K, Schmidt D (2011) Modeling of vapor-liquid equilibrium of gasoline-ethanol blended fuels for flash boiling simulations. Fuel 90(2):665–673
24. Negro S, Brusiani F, Bianchi GM (2011) A numerical model for flash boiling of gasoline-ethanol blends in fuel injector nozzles. SAE Int J Fuels Lubr 4(2):237–256
25. Huang Y, Huang S, Huang R, Hong G (2016) Spray and evaporation characteristics of ethanol and gasoline direct injection in non-evaporating, transition and flash-boiling conditions. Energy Convers Manag 108:68–77
26. Forster H, Zuber N (1954) Growth of a vapor bubble in a superheated liquid. J Appl Phys 25(4):474–478
27. Mohammadein SA, Gouda SA (2006) Temperature distribution in a mixture surrounding a growing vapour bubble. Heat Mass Transf 42(5):359–363
28. Lee HS, Merte H Jr (1996) Spherical vapor bubble growth in uniformly superheated liquids. Int J Heat Mass Transf 39(12):2427–2447
29. Lee HS, Merte H Jr (1996) Hemispherical vapor bubble growth in microgravity: experiments and model. Int J Heat Mass Transf 39(12):2449–2461
30. Robinson AJ, Judd RL (2004) The dynamics of spherical bubble growth. Int J Heat Mass Transf 47(23):5101–5113
31. Xi X, Liu H, Jia M, Xie M, Yin H (2017) A new flash boiling model for single droplet. Int J Heat Mass Transf 107:1129–1137
32. Lien YC (1969) Bubble growth rates at reduced pressure. Doctoral dissertation, Massachusetts Institute of Technology
33. Plesset MS, Zwick SA (1952) A nonsteady heat diffusion problem with spherical symmetry. J Appl Phys 23(1):95–98
34. Plesset MS, Zwick SA (1954) The growth of vapor bubbles in superheated liquids. J Appl Phys 25(4):493–500
35. Prosperetti A, Plesset MS (1978) Vapour-bubble growth in a superheated liquid. J Fluid Mech 85(2):349–368
36. Dalle Donne M, Ferranti MP (1975) The growth of vapor bubbles in superheated sodium. Int J Heat Mass Transf 18(4):477–493
37. Mikic BB, Rohsenow WM, Griffith P (1970) On bubble growth rates. Int J Heat Mass Transf 13(4):657–666
38. Theofanous TG, Patel PD (1976) Universal relations for bubble growth. Int J Heat Mass Transf 19(4):425–429
39. Theofanous T, Biasi L, Isbin HS, Fauske H (1969) A theoretical study on bubble growth in constant and time-dependent pressure fields. Chem Eng Sci 24(5):885–897
40. Board SJ, Duffey RB (1971) Spherical vapour bubble growth in superheated liquids. Chem Eng Sci 26(3):263–274
41. Oza RD, Sinnamon JF (1983) An experimental and analytical study of flash-boiling fuel injection. SAE Trans 92:948–962
42. Oza RD (1984) On the mechanism of flashing injection of initially subcooled fuels. J Fluids Eng 106(1):105–109
43. Reitz RD (1990) A photographic study of flash-boiling atomization. Aerosol Sci Technol 12(3):561–569
44. Senda J, Hojyo Y, Fujimoto H (1994) Modeling on atomization and vaporization process in flash boiling spray. Jsae Rev 15(4):291–296
45. Sher E, Elata C (1977) Spray formation from pressure cans by flashing. Ind Eng Chem Process Des Dev 16(2):237–242
46. Razzaghi M (1989) Droplet size estimation of two-phase flashing jets. Nucl Eng Des 114(1):115–124
47. Plesset MS, Whipple CG (1974) Viscous effects in Rayleigh–Taylor instability. Phys Fluids 17(1):1–7
48. Fedoseev VA (1958) Dispersion of a stream of superheated liquid. Colloid J 20(4):463–466
49. Adachi M, McDonell VG, Tanaka D, Senda J, Fujimoto H (1997) Characterization of fuel vapor concentration inside a flash boiling spray (No. 970871). SAE Technical Paper
50. Kawano D, Goto Y, Odaka M, Senda J (2004) Modeling atomization and vaporization processes of flash-boiling spray (No. 2004-01-0534). SAE Technical Paper
51. Suma S, Koizumi M (1977) Internal boiling atomization by rapid pressure reduction of liquids. Trans Jpn Soc Mech Eng 43(376):4608
52. Zeng Y, Chia-fon FL (2007) Modeling droplet breakup processes under micro-explosion conditions. Proc Combust Inst 31(2):2185–2193

53. Brown R, York JL (1962) Sprays formed by flashing liquid jets. AIChE J 8(2):149–153
54. Lienhard JH, Stephenson JM (1966) Temperature and scale effects upon cavitation and flashing in free and submerged jets. J Basic Eng 88(2):525–531
55. Bushnell DM, Gooderum PB (1969) Measurement of mean drop sizes for sprays from superheated waterjets. J Spacecr Rockets 6(2):197–198
56. Lienhard JH, Day JB (1970) The breakup of superheated liquid jets. J Basic Eng 92(3):515–521
57. Crowe CT, Comfort III WJ (1978) Atomization mechanisms in single-component, two-phase, nozzle flows (No. UCRL-79656 (Rev. 1); CONF-780820-4). California Univ., Livermore (USA). Lawrence Livermore Lab
58. Kitamura Y, Morimitsu H, Takahashi T (1986) Critical superheat for flashing of superheated liquid jets. Ind Eng Chem Fundam 25(2):206–211
59. Zuo B, Gomes AM, Rutland CJ (2000) Modelling superheated fuel sprays and vaporization. Int J Engine Res 1(4):321–336
60. Khan MM, Hélie J, Gorokhovski M, Sheikh NA (2017) Experimental and numerical study of flash boiling in gasoline direct injection sprays. Appl Therm Eng 123:377–389
61. Senecal PK, Schmidt DP, Nouar I, Rutland CJ, Reitz RD, Corradini ML (1999) Modeling high-speed viscous liquid sheet atomization. Int J Multiph Flow 25(6–7):1073–1097
62. VanDerWege BA (1999) The effects of fuel volatility and operating conditions on sprays from pressure-swirl fuel injectors. Doctoral dissertation, Massachusetts Institute of Technology
63. Vanderwege BA, Hochgreb S (1998) The effect of fuel volatility on sprays from high-pressure swirl injectors. Twenty-Seventh Symposium (International) on Combustion/The Combustion Institute, vol 27(2), pp 1865–1871
64. Cleary V, Bowen P, Witlox H (2007) Flashing liquid jets and two-phase droplet dispersion: I. Experiments for derivation of droplet atomisation correlations. J Hazard Mater 142(3):786–796
65. Witlox H, Harper M, Bowen P, Cleary V (2007) Flashing liquid jets and two-phase droplet dispersion: II. Comparison and validation of droplet size and rainout formulations. J Hazard Mater 142(3):797–809
66. Sovani SD, Sojka PE, Lefebvre AH (2001) Effervescent atomization. Prog Energy Combust Sci 27(4):483–521
67. Deich ME, Filippov GA (1970) The gas dynamics of two-phase media (No. FTD-HT-23-188-69). FOREIGN TECHNOLOGY DIV WRIGHT-PATTERSON AFB OHIO
68. Bar-Kohany T, Sher E (2004) Subsonic effervescent atomization: a theoretical approach. At Sprays 14(6):495–510

Bharat Bhatia is a Ph.D. student at Indian Institute of Technology Kanpur. His research interest includes multiphase flows, reactive flow modelling, and direct numerical simulations.

Ashoke De is an Associate Professor at Indian Institute of Technology Kanpur. His research interest includes advanced turbulent combustion modelling, fluid–structure interaction, supersonic flows, combustion instabilities, lattice Boltzmann modelling, and turbulence modelling.